

1 Soundness and Compressive Strength of Portland Cement Blended with 2 Ground Granulated Ferronickel Slag

3 Muhammad Ashiqur Rahman^{*1}, Prabir Kumar Sarker², Faiz Uddin Ahmed Shaikh² and Ashish
4 Kumer Saha¹

5 ¹PhD student, Curtin University, GPO Box U1987, Perth, WA 6845, Australia

6 ²Associate Professor, Curtin University, GPO Box U1987, Perth, WA 6845, Australia

7 Highlights:

- 8 1. Soundness and compressive strength of ferronickel slag (FNS) as SCM were studied.
- 9 2. Effects of FNS on water demand and setting times were similar to those of other SCMs.
- 10 3. The high Mg of FNS present in the form of forsterite ferroan did not increase
11 expansion.
- 12 4. Effect of FNS on strength development is comparable to that of low-calcium fly ash.

13
14 **Abstract:** This paper evaluates the fresh and hardened properties of cement pastes and mortars
15 blended with a ground granulated high-magnesium ferronickel slag (FNS). The main elements of
16 the slag are Silicon (Si), Magnesium (Mg) and Iron (Fe). Test results show that water demand and
17 setting times were not significantly changed by use of the FNS as cement replacement up to 50%.
18 Le-Chatelier soundness test, autoclave expansion test and accelerated curing at 80 °C for 120 days
19 showed no increase of expansion by up to 65% FNS despite its high magnesium content. This is
20 because the Mg was found to be in the form of stable forsterite ferroan that did not take part in the

* Corresponding author.

Tel.: +618 9266 7568; fax: +618 9266 2681

Email addresses: m.rahman24@postgrad.curtin.edu.au (M. Rahman), p.sarker@curtin.edu.au (P.K. Sarker),
S.Ahmed@curtin.edu.au (U.A. Shaikh)

21 hydration and expansive $Mg(OH)_2$ (Brucite) was not found in the scanning electron microscope
22 (SEM) images of the microstructure and powder X-ray diffraction (XRD). The 28-day strength
23 activity index of the FNS was 84%. The 90-day mortar compressive strengths were 93% and 68%
24 of the control specimen for 20% and 50% FNS respectively. Thus the soundness and strength
25 development of the ground FNS were found comparable to those of other commonly used
26 supplementary cementitious materials such as class F fly ash.

27

28 **Keywords:** Blended cement, compressive strength, mortar, ferronickel slag, soundness.

29

30 **1. Introduction**

31 Cement is known as an energy intensive material, which is the conventional binder used
32 for concrete. Concrete is the most widely used construction material because of its versatile
33 properties, availabilities of raw materials, high strength and good durability. However,
34 approximately one tonne of carbon dioxide is emitted to the environment in the production of one
35 tonne of cement [1]. Globally, about 5% to 7% of the carbon footprint is estimated to be related to
36 the production of cement [2]. Thus the reduction of greenhouse gas emission associated with
37 concrete production has become an important consideration in mix design of concrete in the recent
38 years. Besides, the increasing demand of energy, housing and infrastructure development will
39 continue to increase the demand of concrete. Therefore, it is important to increase the use of
40 industrial by-products as supplementary cementing materials (SCMs) in order to reduce the
41 greenhouse gas emission of concrete production.

42

43 At present time, extensive research is focusing on the improvements of concrete properties
44 by using SCMs [3]. The SCMs can be used individually with Portland or blended cement or in
45 different combinations of them which can improve sustainability, economy and various fresh and

46 hardened properties of concrete through hydraulic and pozzolanic actions [4]. The high silica and
47 alumina contents of SCMs can help reduce permeability and improve durability through pozzolanic
48 reactions [5]. Typical examples of SCMs are fly ash, ground granulated blast furnace slag
49 (GGBFS), silica fume, rice husk ash, palm oil fuel ash and natural pozzolans such as calcined clay
50 and calcined shale which are incorporated in concrete as an additive or partial replacement of
51 cement [6-9]. Over the last few decades, the uses of SCMs in concrete have been increased
52 significantly in all over the world. Currently, more than 90% of concrete contains at least one SCM.
53

54 The suitability of using a proprietary ferronickel slag (FNS) as a supplementary
55 cementitious material has been investigated in this study. Ferronickel slag is a by-product of the
56 production of nickel. Some common types of ores used as the source of nickel are pentlandite,
57 pyrrhotite, garnierite, millerite and niccolite. The specific FNS used in this study was produced
58 from garnierite ore found in New Caledonia. The smelter produces about 2.0 Million tonnes of
59 granulated slag every year [10]. The slag is a by-product of the pyro-metallurgical process of the
60 ore in an electric arc furnace at temperatures between 1500 °C and 1600 °C [11]. The molten slag
61 is granulated by rapid cooling using sea-water. It is currently deposited in the plant's premises and
62 there has been a substantial quantity of the slag accumulated over many years despite its use in the
63 local construction works for decades. Raw FNS was ground to fine powder using high energy ball
64 milling for 5.5 hours. The chemical compositions of the FNS are given in Table 1. The sum of
65 SiO_2 , Fe_2O_3 and Al_2O_3 for the FNS is about 65%, which meets the requirement of class C natural
66 pozzolans according to the ASTM C618 -12a Standard [12].
67

68 Sintering of the main elements of FNS namely silicon, magnesium and iron form a stable
69 mineral called forsterite [13-15]. It was shown that periclase (MgO) and amorphous silica combine

70 together at temperatures above 900 °C to form forsterite [14]. Forsterite is a highly stable mineral
 71 with melting point of 1890 °C [14-15]. The chemical compositions and characteristics of the
 72 crystalline and non-crystalline minerals of FNS vary with the type of the ore, smelting temperature
 73 and the cooling condition such as slow cooling by air or rapid cooling by water. Rapid water
 74 cooling produces higher amount of bluish green non crystalline minerals. Chemical compositions
 75 of the nickel slags used by other researchers are also collected in Table 1 for comparison with the
 76 FNS used in this study. A wide variation of the chemical compositions, especially in terms of the
 77 contents of magnesium and iron can be seen in the slags used by different researchers. The FNS
 78 used in this study has the highest magnesium content among all these slags.

79

80 **Table 1. Chemical compositions of FNS used in this study and used by other researchers**

| Oxides | Current Study | Lemonis et al. [16], Katsiotis et al. [17] | Yang et al. [18] | Zhang et al. [19] | Maragkos I. et al. [20] | Komnitas K. et al. [21] | Choi et al. [22] | Dourdounis et al. [23] |
|--------------------------------|---------------|--|------------------|-------------------|-------------------------|-------------------------|------------------|------------------------|
| SiO ₂ | 53.29 | 41.18 | 52.27 | 52.3 | 40.29 | 32.74 | 62.8 | 34.31 |
| Al ₂ O ₃ | 2.67 | 5.98 | 6.19 | 6.2 | 10.11 | 8.32 | 1.95 | 5.73 |
| Fe ₂ O ₃ | 11.9 | 40.02 | 4.2 | 4.2 | 37.69 | 43.83 | 7.13 | 10.33 |
| FeO | - | - | - | - | - | - | - | 37.55 |
| MgO | 31.6 | 7.79 | 26.93 | 26.9 | 5.43 | 2.76 | 24.7 | 1.97 |
| SO ₃ | - | 0.64 | - | - | - | - | 0.03 | |
| CaO | 0.42 | 4.12 | 8.77 | 8.8 | 3.65 | 3.73 | 2.07 | 14.12 |
| Na ₂ O | 0.11 | 0.09 | 0.11 | 0.1 | - | - | 0.13 | - |
| K ₂ O | - | 0.37 | 0.16 | 0.2 | - | - | 0.02 | |
| Cr ₂ O ₃ | 1.08 | 2.75 | 0.37 | 0.4 | 2.58 | 3.07 | - | 3.5 |
| TiO ₂ | - | 0.12 | 0.1 | 0.1 | - | - | - | - |
| ZnO | - | - | 0.02 | <0.1 | - | - | - | - |
| MnO | - | 0.52 | - | - | - | - | - | - |
| NiO | 0.1 | - | 0.03 | <0.1 | 0.09 | 0.1 | - | 0.26 |
| Co ₃ O ₄ | 0.01 | - | - | - | - | 0.02 | - | - |
| CoO | - | - | - | - | - | - | - | - |
| P ₂ O ₅ | - | - | - | - | - | - | - | - |
| S | - | - | - | - | - | 0.18 | - | - |

| | | | | | | | | |
|-----|--------|-------|---|-----|---|------|------|------|
| C | - | - | - | - | - | 0.11 | - | - |
| LOI | - 0.83 | -3.44 | - | 0.5 | - | - | 0.94 | 0.00 |

81

82 Very limited number of studies are available in literature on the use of FNS in concrete.
83 Hydration and leaching study of a low-magnesium FNS up to 20% of the binder showed slightly
84 lower water demand and prolonged setting times [16-17]. Lower compressive strengths at the early
85 ages and about 90% compressive strength at 90 days as compared to the control specimens were
86 reported in these studies. Investigations on geopolymer technology [18-19] showed that the use of
87 20% high-magnesium nickel slag yielded higher compressive strength and lower drying shrinkage.
88 Improved mechanical properties were attributed to the presence of glassy and more silicate phases
89 of the FNS. It was also stated that the slag was much less reactive because of the pyro-metallurgical
90 process at high temperature. Margakos et al. [20] and Komnitas et al. [21] used low-magnesium
91 FNS for synthesis of inorganic polymers. Choi et al [22] studied the effect of a high-magnesium
92 FNS fine aggregate on the alkali-silica reaction of concrete. Dourdounis et al. [23] studied the use
93 of a low-magnesium FNS for the production of high alumina cement. Therefore, it can be seen
94 from the reviews that studies on the use of high-magnesium FNS as a cement replacement are
95 scarce in literature.

96

97 As the slag used in this study has relatively high magnesium content, it is necessary to
98 investigate the effects of this slag on the soundness and strength development of the binder.
99 Therefore, paste and mortar specimens were cast and tested using different proportions of the
100 ground ferronickel slag as a partial replacement of cement. This study has focused on some
101 important properties of the fresh and hardened paste and mortar samples. The fresh properties
102 included the normal consistency and setting times, and the hardened properties included expansions
103 by different test methods, strength activity index and the development of mortar compressive

104 strength with age. X ray diffraction (XRD), scanning electron microscopy (SEM) and energy
105 dispersive X-ray spectra (EDS) tests were conducted on hardened paste samples to have an insight
106 of the reaction products and understand the expansion behaviour shown by the specimens
107 containing the FNS.

108

109 **2. Experimental work**

110 **2.1 Materials**

111 The maximum particle size of the granulated slag was about 5mm. It was ground using a
112 laboratory ball mill to a fineness of 500 m²/kg. The specific surface area of the ground slag was
113 determined using the Blaine's air permeability method according to the ASTM C204-11 Standard
114 [24]. The photographs of the raw slag and the ground slag are shown in Fig. 1. The specific gravity
115 of the ferronickel slag was 2.95, which is similar to that of Portland cement (about 3.15) or other
116 supplementary cementitious materials such as GGBFS (2.90).



117

118

119

120

121

122

Raw ferronickel slag

Ground ferronickel slag

123

Figure 1. Raw and ground ferronickel slag

124

125

126

127

128

129

130

131

132

133

The chemical compositions of the FNS were determined by X-ray fluorescence (XRF) and the elements in terms of their oxides are given in Table 1. Though the XRF results show the Mg content in terms of MgO, an X-ray diffraction (XRD) phase analysis of the FNS showed the presence of magnesium mainly in the form of crystalline forsterite ferroan. The chemical compositions of the cement, fly ash and GGBFS used in the study are given in the Table 2. The Blaine's fineness of the ground FNS, cement, fly ash and GGBFS were 500 m²/kg, 370 m²/kg, 330 m²/kg and 450 m²/kg respectively.

Table 2. Chemical compositions of the cement, fly ash and GGBFS

| Oxides | OPC | Fly ash | GGBFS |
|--------------------------------|-------|---------|-------|
| SiO ₂ | 20.29 | 76.34 | 32.45 |
| Al ₂ O ₃ | 5.48 | 14.72 | 13.56 |
| Fe ₂ O ₃ | 2.85 | 3.69 | 0.82 |
| MgO | 1.24 | 0.54 | 5.10 |
| SO ₃ | 2.49 | 0.11 | 3.20 |
| CaO | 63.11 | 0.60 | 41.22 |
| Na ₂ O | 0.29 | 0.19 | 0.27 |
| K ₂ O | 0.45 | 0.96 | 0.35 |
| Cr ₂ O ₃ | 0.02 | - | - |
| P ₂ O ₅ | 0.17 | 0.10 | 0.03 |
| SrO | 0.05 | - | - |
| TiO ₂ | 0.27 | 0.61 | 0.49 |
| Mn ₂ O ₃ | 0.08 | 0.07 | 0.25 |
| ZnO | 0.04 | - | - |
| LOI | 3.39 | 0.53 | 1.11 |

134

135 The fine aggregate was natural river sand with fineness modulus of 1.95. The specific gravity
136 (SSD) and apparent density of the sand was 2.15 and 2.30 t/m³ respectively. Normal potable tap
137 water was used in mixing of the pastes and mortar mixtures.

138

139 **3. Methodology**

140 A series of tests were conducted to assess the fresh properties of cement paste blended with
141 the FNS. The test results were compared with those of the control mixtures without the slag.
142 Comparison was also made with the results of cement paste mixtures blended with fly ash (FA)
143 and ground granulated blast furnace slag (GGBFS) as two other commonly used supplementary
144 cementitious materials. The properties include normal consistency, initial and final setting times,
145 strength activity index and soundness by different methods. Compressive strength development of
146 mortar specimens containing ferronickel slag was also determined. Powder X-Ray diffraction
147 (XRD) phase analysis and investigation of the microstructure by scanning electron microscopy
148 (SEM) image and energy dispersive spectra (EDS) were carried out to have an insight into the
149 reaction product of the ferronickel slag in cement paste. The test methods, mixture proportions and
150 specimens for each test are described in the following sections.

151

152 ***3.1 Normal consistency and setting time***

153 The knowledge of the setting time of a cementitious mixture is required in order to
154 determine the available time for mixing, transporting, placing and compacting the concrete
155 effectively. Setting time tests are used to characterize how a particular cementitious paste sets. It
156 is affected by a number of factors such as the fineness and chemical compositions of the
157 cementitious materials, water-binder ratio, and the admixtures if used. Setting time and soundness
158 properties are determined at a specified consistency rather than certain water-binder ratio [25].

159 Therefore, the water content for normal consistency is determined as a pre-requisite for the setting
160 time and soundness tests.

161
162 Commercial GGBFS can be used up to 65% cement replacement and 20% is considered as
163 the lower range of SCM dosage. Hence, the ferronickel slag was used from 20% to 65% by weight
164 as partial replacement of cement. The normal consistencies and setting times of the mixtures were
165 determined in accordance with the Australian Standards AS 2350.3 and AS 2350.4 respectively.
166 The tests were conducted on freshly mixed pastes in the laboratory at a relative humidity of $70 \pm$
167 10% and temperature of 23 ± 2 °C.

168
169 **3.2 Strength activity index**

170 Strength activity index is defined as the ratio of the strength of 20% ferronickel slag-
171 blended cement mortar to the strength of the reference cement mortar at a specific age. The control
172 cement mortar mixture consisted of 500g of cement, 1375g of sand and 242g of water as specified
173 in the ASTM C311M Standard [26]. The ferronickel slag blended cement mortar mixture contained
174 400g cement, 100g ferronickel slag, 1375g sand and 242g of water. Since the water demand for
175 normal consistency of the 20% ferronickel slag blended paste was same as that of the control
176 cement paste, the same water contents were used in both the mortar mixtures. Cube specimens of
177 50mm sides were prepared and tested in accordance with the ASTM C311M Standard [26]. After
178 casting, the specimens were placed in a moist room at 23 ± 2 °C for 24 h. The specimens were then
179 demoulded and cured in lime saturated water until tested for compressive strengths at the ages of
180 7 and 28 days.

181
182

183 3.3 Soundness

184 As shown in Table 1, the magnesium content of the FNS obtained by XRF analysis
185 expressed in terms of its oxide is about 32%. According to AS 3582.2 [27-28], the value of MgO
186 in SCMs should be less than 15%. However, the reactivity of MgO depends on its calcination
187 temperature. MgO can be classified in three temperature categories of calcination: a) lightly burnt
188 MgO (850-1200 °C), hydration takes place within 180 days b) heavily burnt MgO (1500-1800 °C),
189 hydration can be up to 1000 days and c) dead burnt MgO, Periclase (>1800 °C), hydration can
190 proceed up to 6-8 years [29]. The higher the burning temperature, the smaller is the magnitude of
191 early-age expansion and the longer the MgO hydration process lasts. When MgO hydrates, it
192 produces Mg(OH)₂ (Brucite), which increases the volume by 17% [30]. The unsoundness caused
193 by the excessive volume changes is usually accompanied by cracking and strength loss.

194
195 However, it should be noted that magnesium may not always be harmful for concrete
196 depending on how it is chemically bound in the slag. XRD results of the FNS showed that the
197 magnesium is present in the form of crystalline forsterite ferroan rather than in the form of MgO.
198 Therefore, the actual effect of the high magnesium content of the slag on expansion needs to be
199 determined by expansion tests. Thus, the soundness of the ferronickel slag blended cement pastes
200 has been evaluated using the well-known Le-Chatelier soundness test, autoclave expansion test and
201 an accelerated heat curing test.

202
203 The Le-Chatelier soundness test was carried out in accordance with the Australian Standard
204 AS2350.5 [31]. Three samples were prepared for each type of mixture and an average value of the
205 measured expansions is reported. The paste samples were prepared at normal consistency by
206 replacing 0% to 65% of cement by the FNS.

207
208 The autoclave expansion was determined in accordance with the Australian Standard AS
209 3583.4 [32]. The paste specimens used for this experiment were prisms of 25 mm square by 285
210 mm length, having a 250 mm effective gauge length. A paste of normal consistency was prepared,
211 moulded and cured for 24 hours in a moist cupboard. After curing, the specimens were demoulded
212 and the initial lengths were measured. The specimens were then placed in the autoclave, containing
213 water, to maintain an atmosphere of saturated steam. The temperature of the autoclave was raised
214 at a rate that brought the steam pressure to 2000 kPa in 45 min to 75 min. A pressure of 2000 ± 70
215 kPa was maintained within the autoclave for 3 hours. Afterwards, the specimens were cooled down
216 to room temperature and the changes of lengths were measured.

217
218 It was reported that curing at elevated temperature such as 80 °C could accelerate the
219 hydration of lightly burnt (1000-1250 °C) MgO and complete hydration would be achieved within
220 30 days [29]. Therefore, accelerated heat curing tests were conducted to further investigate the
221 expansion characteristics of the control and the FNS blended cement pastes. The specimens were
222 of the same size as those used for the autoclave expansion test and were cast with 30% and 50%
223 FNS as cement replacement. Another batch of samples was cast with the inclusion of 5% and 10%
224 MgO (minimum 95% Magnesia) with cement in order to compare the expansions of the specimens
225 containing the FNS and those with reactive MgO. One set of the specimens were cured at 80 °C in
226 water for 120 days and another set was cured in water at ambient temperature to compare the
227 expansions under normal and accelerated conditions. Three identical specimens were tested for
228 each condition and the average value of the expansions is reported.

229

230

231 **3.4 Compressive Strength of Mortar**

232 The mortar mixtures consisted of one part of binder and three parts of sand by mass with a
233 water-binder ratio of 0.50. Ferronickel slag was used to replace 20, 30, 40 and 50% of cement in
234 the mixtures. Since the calcium content of the FNS was very low (0.42%), the cement replacement
235 was limited to 50% considering that higher percentages of FNS would result in very low strength.
236 The specimens were cured in water at 23 ± 2 °C and compression tests were conducted following
237 the ASTM C109 Standard [33]. Three samples were tested for each mix at 3, 14 and 28 days of age
238 and the average compressive strength is reported.

239

240 **4. Results and discussion**

241 **4.1 Normal consistency and setting time**

242 The normal consistency results of the pastes containing up to 65% ferronickel slag are
243 shown in Fig. 2. The water contents required to achieve the normal consistency of the pastes are
244 plotted against the percentage of ferronickel slag in this figure.

245

246

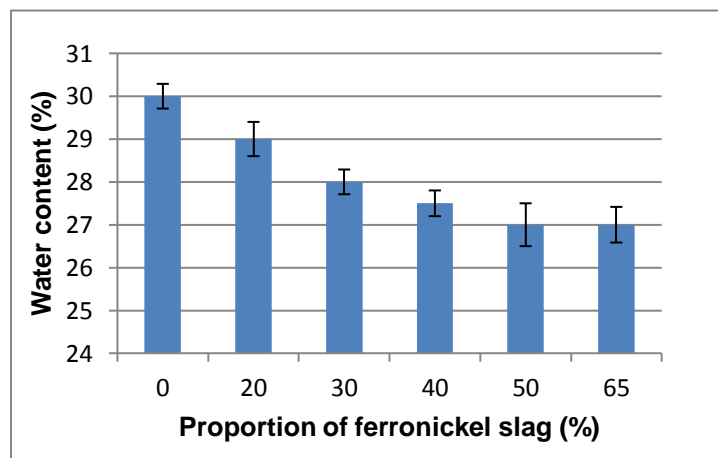
247

248

249

250

251



252 **Figure 2. Water contents for normal consistency of paste containing different percentages**
253 **of ferronickel slag**

254

255 The results in Fig. 2 shows that the amount of water required for normal consistency of the
256 paste slightly decreased with the inclusion of ferronickel slag. The water content required for
257 normal consistency of the control mixture was 30% and that of the mixtures with ferronickel slag
258 varied from 29% to 27%. Therefore, the required water content decreased from 30% to 27% with
259 the inclusion of 65% ferronickel slag in the paste. The ratios of the water requirement of the control
260 mix to those of the mixes containing 30% and 65% ferronickel slag are 1.07 and 1.11, respectively.
261 ASTM Standard C618.12a [12] recommends the maximum ratios of 1.05 and 1.15 for fly ash and
262 natural pozzolans respectively. Thus, the water requirements of ferronickel slag are comparable to
263 those of other supplementary cementitious materials. The observed decrease in water requirement
264 of the ferronickel slag is attributed to its low water absorption characteristics and the inert
265 behaviour at the initial stage of mixing.

266

267

268

269

270

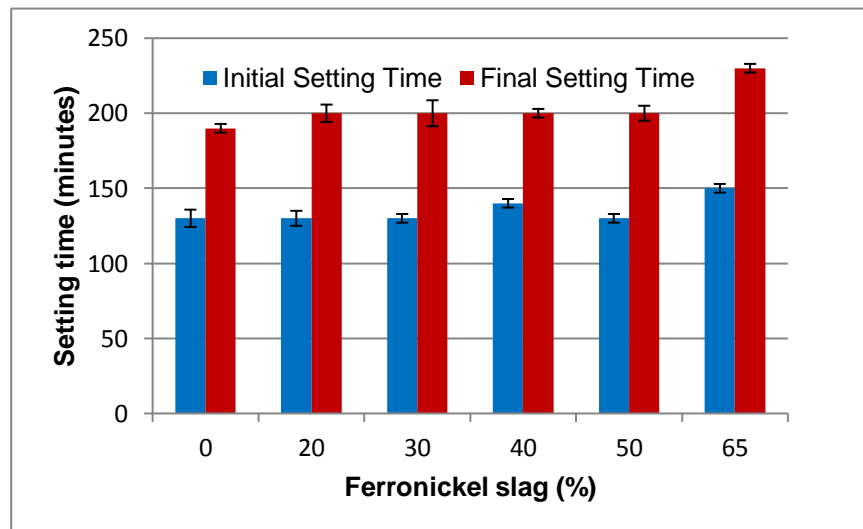
271

272

273

274

275



276

277

Figure 3. Variation of setting times with the percentage of ferronickel slag

278

279

280

The initial and final setting time results of the control cement paste and the mixtures with up to 65% ferronickel slag are shown in Fig. 3. It can be seen that the initial setting times of the

281 mixtures varied from 130 minutes to 150 minutes and the final setting time varied from 190 minutes
282 to 230 minutes. According to ASTM C150 [34] specification, the initial setting time shall not be
283 less than 45 minutes. However, an initial setting time of at least 90 minutes is usually preferred in
284 practice. A very long final setting time is not usually preferred because this may cause large
285 expenditures on the formwork. Therefore, the initial and final setting times of the mixtures
286 containing up to 65% ferronickel slag are considered suitable for usual applications of concrete.

287
288 No significant difference in the setting times was observed due to incorporation of the
289 ground ferronickel slag as a cement replacement up to 50%. At the cement replacement level of
290 65%, the ferronickel slag was found to retard the initial setting time by 20 minutes and final setting
291 time by 40 minutes. It is usually observed that increasing the amount of supplementary
292 cementitious materials such as silica fume, fly ash and GGBFS retards the setting time of concrete
293 [35]. Cement replacement by GGBFS at a rate more than 40% was shown to significantly increase
294 the setting time [36].

295
296 The normal setting time of Portland cement is related to the hydration of C_3S and C_3A , and
297 the formations of CSH gel and ettringite [37]. High level of cement replacement causes reduction
298 of the hydrated products from C_3S and C_3A . Also, the increased percentage of cement replacement
299 by SCMs causes the separation distance between hydrated cement particles to increase, which
300 eventually delays the formation of interlocking network between the particles. It should also be
301 noted that the ferronickel slag has a very low (0.42%) calcium content. Thus, the setting time is
302 increased at a high percentage of cement replacement such as 65% by the low calcium ferronickel
303 slag.

304

305 **4.2 Strength activity index**

306 The pozzolanicity of the ferronickel slag was quantified by its strength activity index. The
307 strength activity index of any material depends on the surface area, particle size distribution and
308 silica content. The strength activity index can be increased by reducing the particle size thus
309 increasing the fineness. The average compressive strengths obtained from three specimens were
310 used to determine the strength activity index. The results are given in Table 3.

311

312 **Table 3. Strength activity index of ferronickel slag**

| SI No | Composition | Mean 7 days strength (MPa) | Mean 28 days strength (MPa) | Strength activity index | |
|-------|-------------|----------------------------|-----------------------------|-------------------------|---------|
| | | | | 7 days | 28 days |
| 1 | Control | 31 | 37 | 74% | 84% |
| 2 | 20% FNS | 23 | 31 | | |

313

314 Table 3 shows that the strength activity indices for 7 days and 28 days were found 74% and
315 84% respectively. ASTM C618-08a [38] recommends a minimum strength activity index of 75%
316 for fly ash and natural pozzolans at 7 or 28 days. Since the value for the ferronickel slag at 28 days
317 is above 75% and that at 7 days is very close to 75%, the effect of the ferronickel slag on strength
318 development may be considered comparable to those of other supplementary cementitious
319 materials.

320

321 **4.3 Le-Chatelier soundness**

322 The Le-Chatelier expansion results are plotted against the percentage of ferronickel slag in
323 Fig. 4. Expansions of two additional mixtures containing 40% fly ash and 40% GGBFS were also
324 tested for comparison with the expansion of the mixture of 40% ferronickel slag. Besides, two other
325 types of samples were prepared using 5% MgO and 10% MgO with the FNS and cement to
326 investigate the effect of reactive MgO on the expansion.

327

328

329

330

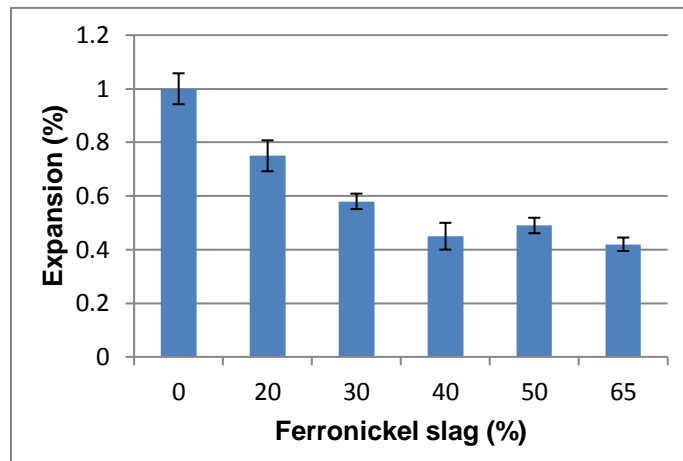
331

332

333

334

335



336

Figure 4. Variation of expansion with the percentages of ferronickel slag

337

338

339

340

341

342

343

It is observed from the results that the Le-Chatelier expansion of the mixtures containing 0% to 65% ferronickel slag varied between 0.42% and 1%. These values are well below 5%, which is specified as the limiting value of Le-Chatelier expansion in the Australian Standard [39]. It can be seen from Fig. 4 that the values generally decreased with the increase of cement replacement by the slag. The value decreased from 0.75% to 0.42% when the cement replacement increased from 20% to 65%.

344

345

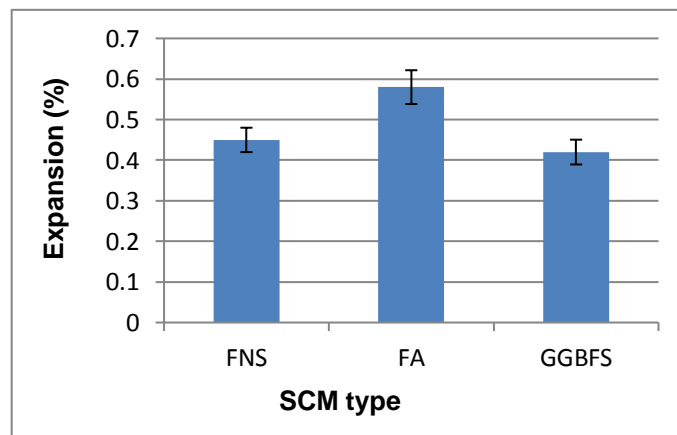
346

347

348

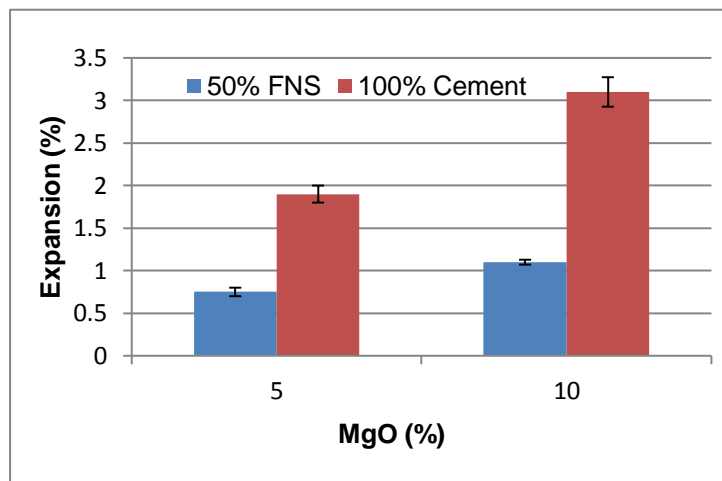
349

350



351 **Figure 5. Le-Chatelier expansions of pastes containing 40% FNS, 40% fly ash and 40%**
352 **GGBFS**

353 Fig. 5 shows the Le-Chatelier expansions of the mixtures with 40% cement replacements
354 by the ferronickel slag, class F fly ash and GGBFS. The mean expansions of the specimens with
355 40% GGBFS, 40% ferronickel slag and 40% fly ash were 0.42%, 0.45% and 0.58% respectively.
356 These values are well below the 5% expansion limit of the Australian Standard [39]. Though the
357 ground FNS had the highest fineness (500 m²/kg) as compared to the fly ash (330 m²/kg) and
358 GGBFS (450 m²/kg), the reaction of the FNS did not cause excessive expansion of the specimens.
359 Thus the Le-Chatelier expansion of the mixture containing 40% ferronickel slag is similar to those
360 of the mixtures containing the same percentage of other common supplementary cementitious
361 materials such as fly ash and GGBFS.



362
363
364
365
366
367
368
369
370
371 **Figure 6. Le-Chatelier expansions of pastes containing 5% MgO and 10% MgO with and**
372 **without ferronickel slag**

373
374 Expansions of four other mixtures containing 5% or 10% reactive MgO was also measured
375 in order to evaluate the sensitivity of the Le-Chatelier test to the expansions caused by the reaction
376 product of reactive MgO. The MgO powder was added to the mixtures of 100% cement or 50%

377 cement and 50% ferronickel slag. The expansions of these four mixtures are shown in Fig. 6. When
378 reactive MgO was added to the FNS blended cement mixtures, the expansion was increased with
379 the increase of MgO. This is expected because of the expansion caused by formation of $Mg(OH)_2$
380 by hydration of MgO. As shown in the figure, expansion of the mixture with 10% MgO and
381 without any FNS was 3.1%. The expansions of the mixtures with 50% ferronickel slag were less
382 than those of the corresponding mixtures without ferronickel slag. This is because of the less lime
383 available in the mixtures with 50% ferronickel slag as cement replacements. This indicates that the
384 ferronickel slag did not produce expansive reaction product similar to that produced by reactive
385 MgO.

386
387 Thus, the Le-Chatelier expansions of the pastes containing ferronickel slag up to 65% were
388 found well below the 5% limit of the Australian Standard and were less than that of the control
389 mixture. Expansion of the mixtures containing 40% FNS is comparable with expansions of the
390 mixtures containing same percentage of other common supplementary cementitious materials such
391 as fly ash and GGBFS.

392
393 **4.4 Autoclave expansion**

394 The autoclave expansion tests were conducted on specimens containing 0%, 20%, 30%,
395 40% and 50% ferronickel slag as cement replacement. The expansion results are given in Table 4.
396 No cracks, disintegration or warping were observed in the specimens after completion of the tests.

397
398 **Table 4. Autoclave expansion of ferronickel slag blended mixtures**

| FNS content (%) | Autoclave expansion (%) |
|------------------------|--------------------------------|
| 0 | 0.08 |
| 20 | 0.01 |
| 30 | 0.06 |

399

| | |
|----|------|
| 40 | 0.03 |
| 50 | 0.08 |

400

401

402

403

404

405

406

407

408

409

410

411

412

413

414

415 ***4.5 Expansion by accelerated heat curing***

416

417

418

419

420

421

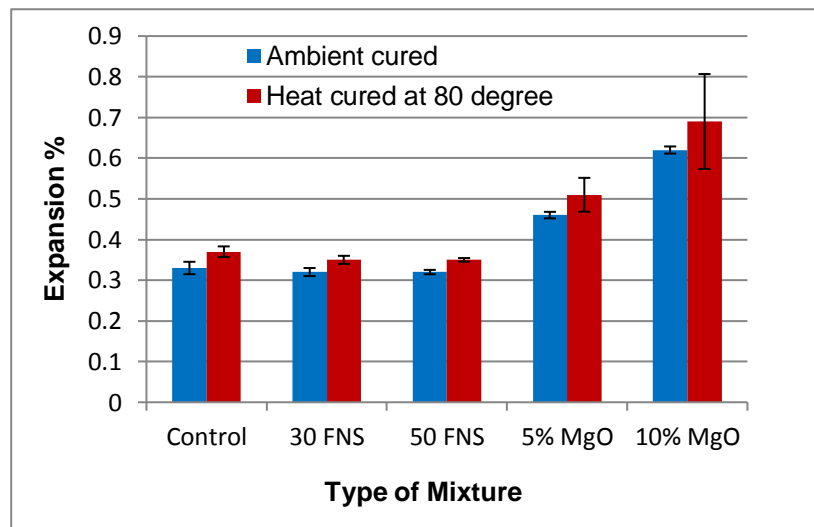
422

423

The results show that the autoclave expansion values were scattered between 0.01% and 0.08% with no definite trend for the increase of the ferronickel slag up to 50%. ASTM Standards C150 [40] and C618-98 [41] limit the autoclave expansion of a cement or blended mix by 0.8%. Therefore, the expansions of these mixtures are very small as compared to the limit set by the ASTM Standards. The expansion in cement or any blended mixture occurs due to the presence of free lime or magnesia (Periclase). The autoclave test is especially designed for measuring the expansion due to periclase. The results do not show any increase in the expansion by the increase of the ferronickel slag in the mixture. This is because the magnesium present in the ferronickel slag is in the form of forsterite rather than periclase. Thus, the autoclave expansion is not increased by the ferronickel slag.

The changes in length of the specimens were measured weekly for 120 days. The expansion test results of the specimens after 120 days of curing in ambient condition and in accelerated heat curing at 80 °C are shown in Fig. 7. It can be seen that 120-day expansion of the ambient-cured control specimen was 0.33% and that of the specimens with either 30% or 50% ferronickel slag was 0.32%. Similarly, the expansion of the heat-cured control specimen was 0.37% and that of the specimens containing ferronickel slag was 0.35%. Thus, the 120-day expansions of the specimens containing ferronickel slag were similar to that of the control specimen. Generally, the heat curing at 80 °C increased expansion of the specimens with or without ferronickel slag. The results show

424 that the specimens containing MgO have higher expansions as compared with the control
 425 specimens and the specimens containing ferronickel slag. The expansions of the ambient-cured
 426 specimens with 5% MgO and 10% MgO were 0.46% and 0.62% respectively. Thus, the expansion
 427 increased by about 39% and 94% by the use of 5% and 10% reactive MgO. Similarly, 38% and
 428 86% increases in expansions of the specimens were also observed by the use of 5% and 10% MgO
 429 for heat curing condition. Therefore, while the use of reactive MgO increased the expansion, the
 430 use of ground ferronickel slag up to 50% did not increase expansion as compared to that of the
 431 control specimens. This shows the difference between the reactivity of the Mg in MgO and that in
 432 the FNS. Thus the effect of ferronickel slag on expansion in these tests is similar to those shown
 433 by the Le-Chattelier test. Generally, the use of ferronickel slag as a cement replacement did not
 434 increase expansion as observed by the results of Le-Chattelier soundness test, autoclave expansion
 435 test and the accelerated heat curing test.

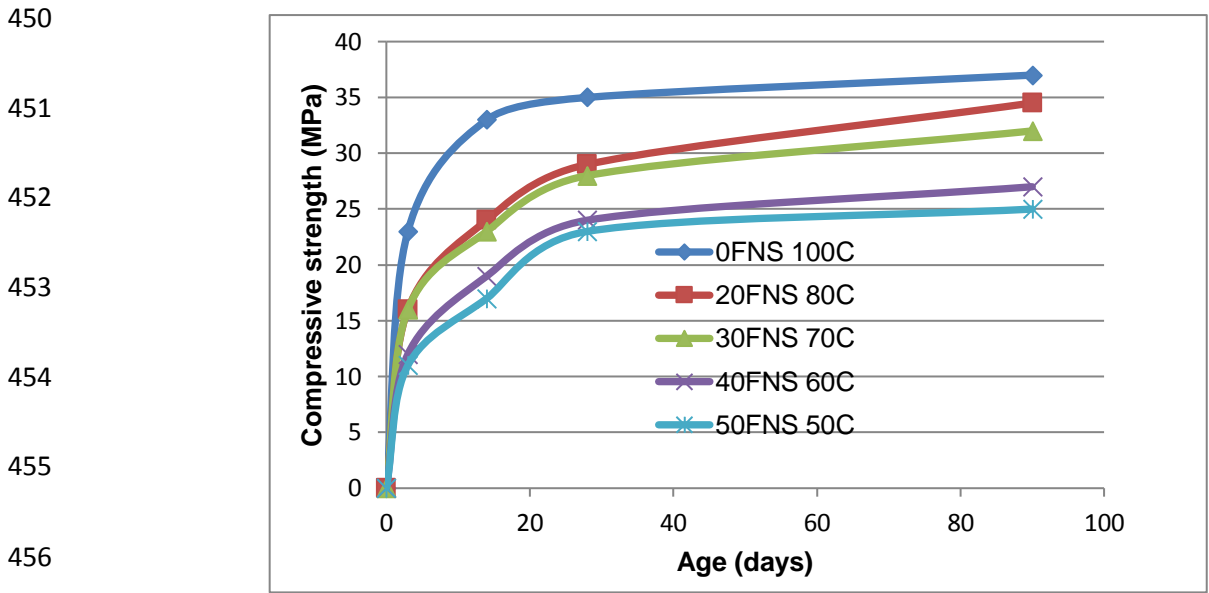


445 **Figure 7. Ambient and heat cured expansion test results**

446

447 **4.6 Compressive strength of mortar specimens**

448 The strength developments of mortar specimens containing 0% to 50% ferronickel slag as
449 cement replacement are shown in Fig. 8.



457 **Figure 8. Compressive strength of mortars containing different percentages of ferronickel**
458 **slag as cement replacement**

459
460 It can be seen from the figure that strengths of the mixtures were decreased at the early ages
461 by use of the ferronickel slag as cement replacement. The rates of strength development of the
462 ferronickel slag blended mixes were higher during 14 to 28 days as compared to that of the control
463 mix. The strength development of the ferronickel slag blended mortar mixtures showed increasing
464 trend up to the age of 90 days. The control mortars of 100% cement developed to 35 MPa and 37
465 MPa strengths at 28 and 90 days respectively. The specimens with 20% and 50% ferronickel slag
466 gained compressive strengths of 93% and 67% as compared with the control specimens at 90 days.
467 Higher cement replacement by the slag resulted in lower strengths, as expected. Thus, the strength
468 development behaviours of ferronickel slag blended mixtures are similar to the general behaviour
469 of concrete containing pozzolanic materials such as class F fly ash.

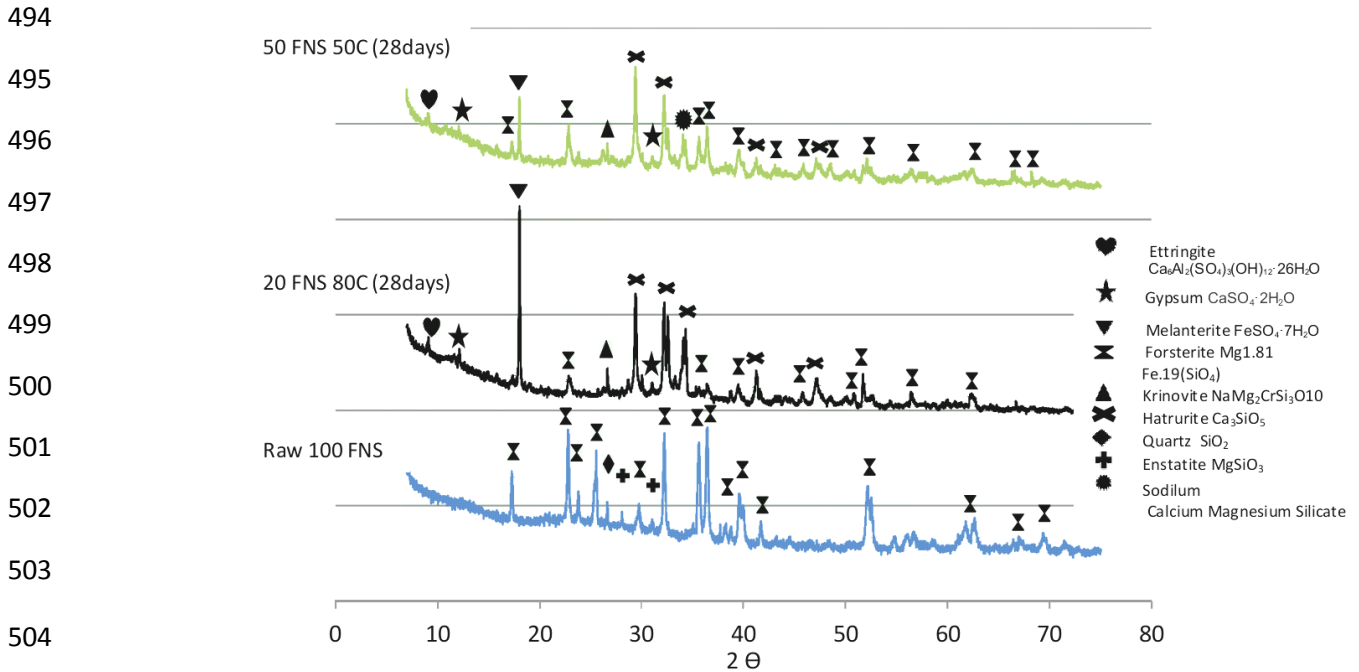
470

471

472 ***4.7 Phase identification by XRD***

473 The formation of different phases by the hydration process was identified using quantitative
474 XRD analysis. The XRD results of the raw ferronickel slag and the specimens with 20% ferronickel
475 slag and 50% ferronickel slag are shown in Fig.9. It is evident from the figure that the major
476 crystalline components in raw ferronickel slag were forsterite ferroan with very small amount of
477 quartz and enstatite. The quantitative analysis showed that raw ferronickel slag contained about 48
478 wt% forsterite ferroan, 2.2 wt% enstatite and 0.4 wt% quartz. The amorphous contents of the FNS
479 are about 50%. Most of the silica is present in amorphous phase rather than in crystalline form.
480 This amorphous silica has participated in the pozzolanic reactions and contributed to the late-age
481 strength development of the mixtures containing ferronickel slag, as shown in Figure 8. In Fig.9,
482 cement mineral hatrurite and the FNS mineral forsterite can be observed in both the paste samples
483 containing ferronickel slag. It can be seen that the intensity of the peaks from the forsterite ferroan,
484 which is contributed by the ferronickel slag, is higher in the sample with 50% ferronickel slag as
485 compared to that of the sample with 20% ferronickel slag. This means that the magnesium
486 containing crystalline phase of ferronickel slag is stable in the hydration process. Since no Brucite
487 was identified in the XRD, the magnesium of the FNS did not take part in the reaction process and
488 it did not contribute to the expansion of the specimens. For this reason, the expansions determined
489 by the Le-Chatelier test, autoclave test and extended heat curing test of the specimens containing
490 ferronickel slag were not higher than those of the control specimens despite the high magnesium
491 content of the slag. The other hydration products found were melanterite and small amounts of
492 ettringite and gypsum.

493



505 **Figure 9. Phase analysis of raw FNS and FNS blended cement pastes by XRD**

506

507 **4.8 Microstructure observation by SEM and EDS**

508 Further to the XRD, the microstructures of hardened paste specimens were investigated by

509 SEM images and EDS in order to identify if there was any expansive Brucite present in the

510 specimens containing 20% and 50% ferronickel slag. Figure 10(a) shows the SEM image and

511 corresponding EDS of the specimen with 20% FNS and Fig. 10(b) shows the SEM image and

512 corresponding EDS of the specimen containing 50% FNS. Generally, a compact microstructure

513 could be observed in both the specimens. It was shown by several researchers [42-45] that the

514 formation of Brucite or $\text{Mg}(\text{OH})_2$ is identified as hexagonal plate shaped crystals that may be often

515 found agglomerated in spherical shaped morphology when observed by SEM. This type of

516 morphological shapes were not found in the SEM images as shown in Figs. 10(a) and 10(b). Thus

517 no $\text{Mg}(\text{OH})_2$ was visible in SEM images of the specimens containing 20% and 50% FNS. This

518 observation is consistent with the XRD results shown in Fig.9 that no $\text{Mg}(\text{OH})_2$ was found in the

519 powder samples. As shown in Figs. 10(a) and 10(b), the EDS identified the presence of mainly Mg,

520 Si, O, Fe and Ca in both cases. These elements refer to the formation of calcium silicate hydrate
521 (C-S-H) and the stable forsterite ferroan phase of the FNS. The ratio of Mg : Si for 20% and 50%
522 FNS were found as 0.70 and 0.75 respectively. The amorphous silica of the FNS participated in
523 pozzolanic reaction to continue the strength gain as shown in Fig.8.

524

525

526

527

528

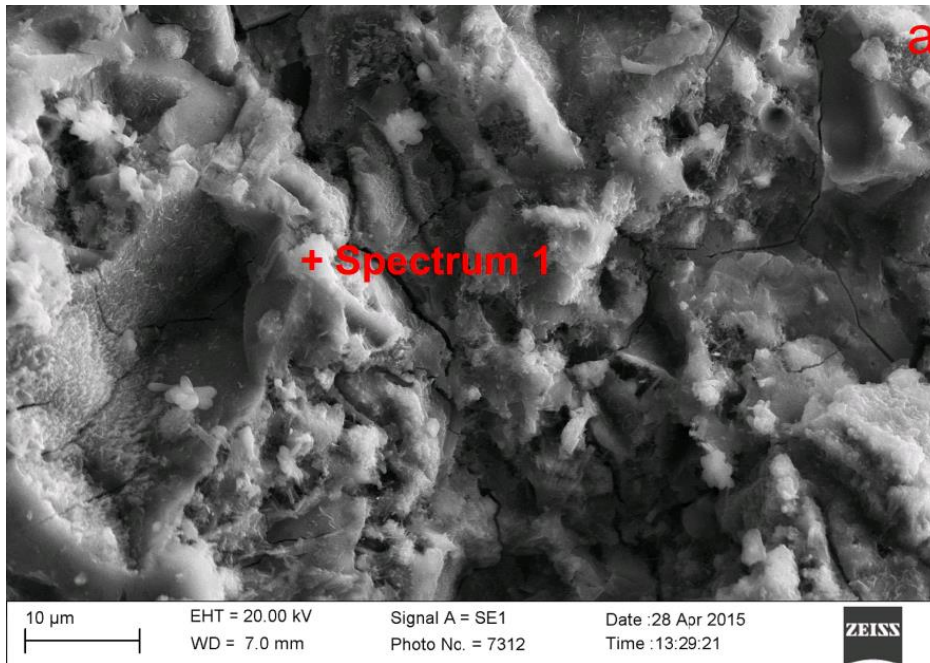
529

530

531

532

533



534

535

536

537

538

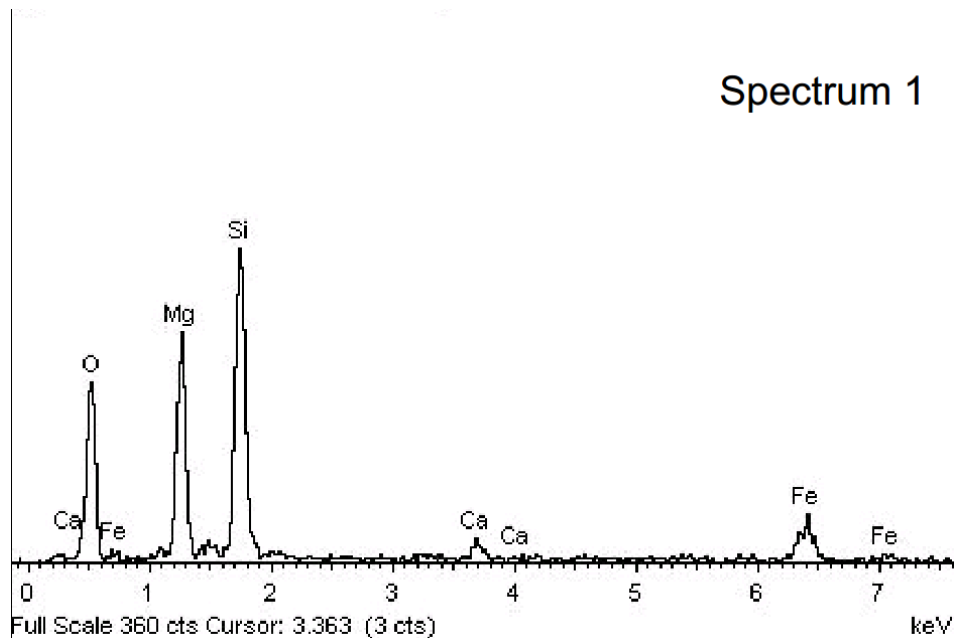
539

540

541

542

543



544
545
546
547
548
549
550
551
552
553
554
555
556
557
558
559
560
561
562
563
564
565
566
567

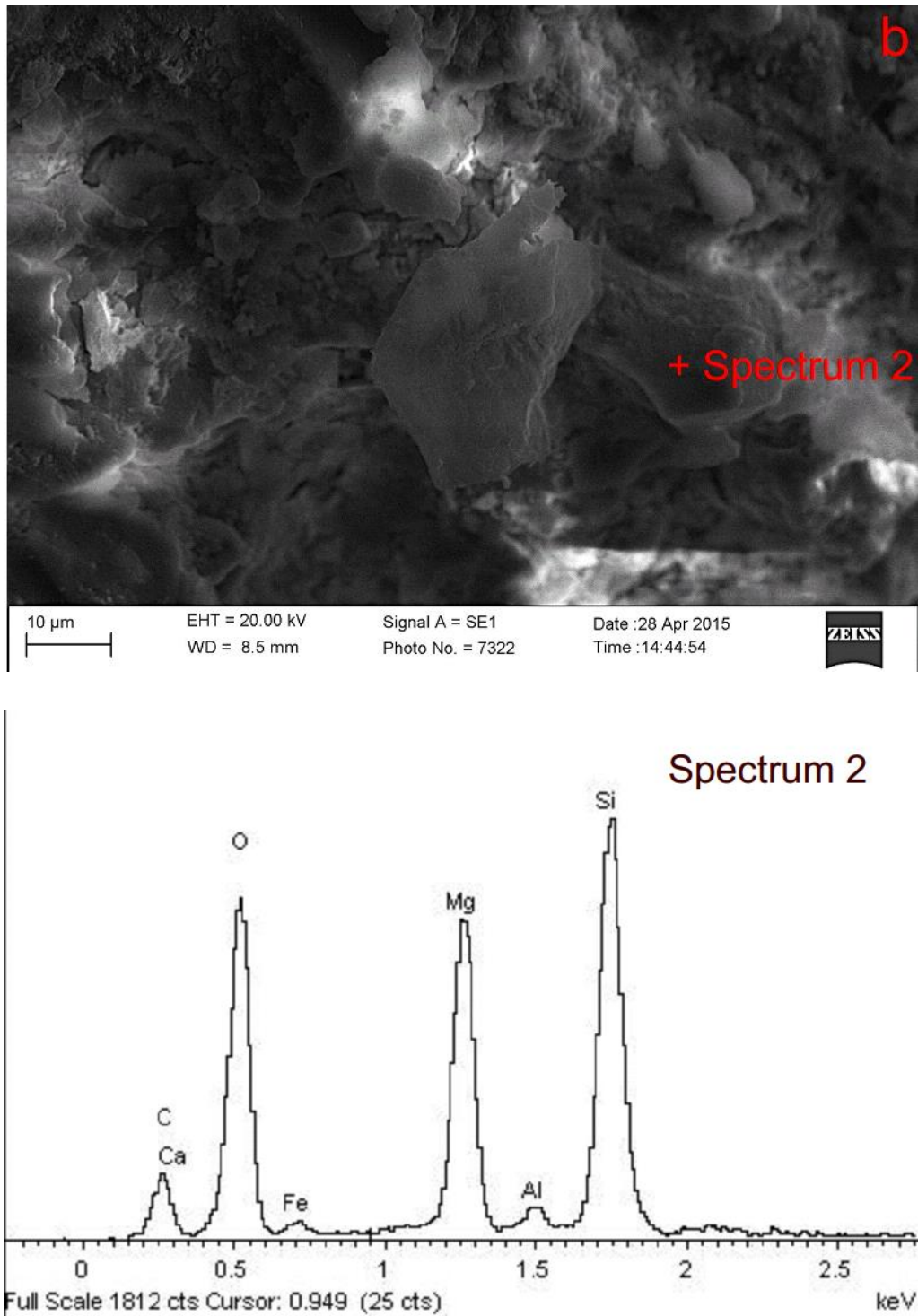


Figure 10. SEM and EDS of hardened paste samples containing 20% (a) and 50% (b) ferronickel slag.

568 **5. Conclusions**

569 This paper presents the fresh and hardened properties of cement paste and mortar specimens
570 containing a high-magnesium ferronickel slag (FNS) as a partial replacement of cement. Water
571 demand and setting times were not significantly affected by the FNS when used up to 50% in the
572 binder. The strength activity indices of the slag at 7 and 28 days were 74% and 84% respectively.
573 No negative effect on the expansion was shown by the slag in the Le-Chatelier, autoclave and
574 extended heat curing tests. The expansions of the specimens with the FNS were less than those for
575 pure cement paste specimens and specimens containing 5% or 10% reactive MgO. This is because
576 of less free lime available in the mixes containing FNS as cement replacement. The expansions
577 were well below the 5% and 0.8% limits set by Standards for the Le-Chatelier and autoclave tests
578 respectively. The 90-day mortar compressive strength was reduced from 37 MPa to 35 MPa by
579 20% FNS and to 25 MPa by 50% FNS. The XRD, SEM and EDS analysis showed no trace of
580 $\text{Mg}(\text{OH})_2$ in the hydration product though the FNS had a high magnesium content. This is because
581 the magnesium was present in the form of stable forsterite ferroan as shown by the XRD results.
582 The amorphous silica present in the slag contributed to the late-age strength development of the
583 specimens. Thus, the soundness and compressive strength development of the ground ferronickel
584 slag was found comparable to those of other commonly used supplementary cementitious materials
585 such as class F fly ash.

586

587 **6. Acknowledgement**

588

589 This research was funded and supported by SLN, New Caledonia. The authors gratefully
590 acknowledge the contribution and continuous support from SLN through its research department
591 and its former consultant, Mr. D.J. Sassoon Gubbay. The authors are grateful to
592 Dr. Michael G Remias (BGC-Cemtech Manager, Western Australia) for his continuous support to

593 the work. The authors also acknowledge the use of Curtin University's Microscopy &
594 Microanalysis Facility, whose instrumentation has been partially funded by the University, State
595 and Commonwealth Governments.

596

597 **7. References**

598

599 [1] Mehta, P. K. 2001. Reducing the environmental impact of concrete, *Concrete International*.
600 23(6), 61-66.

601 [2] Malhotra, V.M., 2000. Role of supplementary cementing materials in reducing greenhouse gas
602 emissions. In: Gjorv, O.E., Sakai, K. (Eds.), *Concrete technology for a sustainable development in*
603 *the 21st Century*. E&FN Spon, London, 226-235.

604 [3] Muhl, A., 2003. The use of supplementary cementing materials in residential concrete. Master's
605 thesis, University of Toronto.

606 [4] CSA A3001-03, 2003. Cementitious materials for use in concrete. National standards of
607 Canada.

608 [5] Aprianti S, E., 2016. A huge number of artificial waste material can be supplementary
609 cementitious material (SCM) for concrete production - a review part II. *Journal of Cleaner*
610 *Production*, Article in Press.

611 [6] Muhmood, L., Vitta, S., Venkateswaran, D., 2009. Cementitious and pozzolanic behavior of
612 electric arc furnace steel slags. *Cem. Concr. Res.* 39, 102-109.

613 [7] Sata, V., Jaturapitakkul, C., Kiattikomol, K., 2007. Influence of pozzolan from various by-
614 product materials on mechanical properties of high-strength concrete. *Constr. Build. Mater.* 21 (7),
615 1589-1598

- 616 [8] Sajedi, F., Razak, H.A., Mahmud, H.B., Shafigh, P., 2012. Relationships between compressive
617 strength of cement slag mortars under air and water curing re-gimes. *Constr. Build. Mater.* 31, 188-
618 196.
- 619 [9] Lilkov, V., Rostovsky, I., Petrov, O., Tzanetanova, Y., Savov, P., 2014. Long term study of
620 hardened cement pastes containing silica fume and fly ash. *Constr. Build. Mater.* 60, 48-56.
- 621 [10] Le Nickel – SLN, FNS: a promising construction material for the Pacific Region. Available
622 at:<http://sln.nc/sites/default/files/flippingbook/slnslg/fichiers/assets/common/downloads/publicati>
623 on.pdf, Accessed on 07 January, 2017.
- 624 [11] Saha, A.K., Sarker, P.K., 2016. Expansion due to alkali-silica reaction of ferronickel slag fine
625 aggregate in OPC and blended cement mortars. *Constr. Build. Mater.* 123, 135-142.
- 626 [12] ASTM C618-12a, 2012. Standard specification for Coal Fly Ash and Raw or Calcined Natural
627 Pozzolan for Use in Concrete. ASTM International.
- 628 [13] Wang , Z.J., Ni, W. et al., 2010. Crystallization behavior of glass ceramics prepared from the
629 mixture of nickel slag, blast furnace slag and quartz sand. *Journal of Non-Crystalline Solids.* 356,
630 1554–1558.
- 631 [14] Kosanovic, C., Stubicar, N. et al., 2005. Synthesis of a forsterite powder by combined ball
632 milling and thermal treatment. *Journal of Alloys and Compounds.* 389, 306–309.
- 633 [15] Maghsoudlu, M.S.A., Ebadzadeh, T. et al. 2016. Synthesis and sintering of nano-sized
634 forsterite prepared by short mechanochemical activation process. *Journal of Alloys and*
635 *Compounds.* 678, 290-296.
- 636 [16] Lemonis, N., Tsakiridis, P.E. et al., 2015. Hydration study of ternary blended cements
637 containing ferronickel slag and natural pozzolan. *Constr. Build. Mater.* 81, 130-139.

- 638 [17] Katsiotis, N.S., Tsakiridis, P.E. et al., 2015. Utilization of ferronickel slag as additive in
639 Portland cement: A hydration leaching study. *Waste and Biomass Valorization*. 6(2), DOI:
640 10.1007/s12649-015-9346-7.
- 641 [18] Yang, T., Yao, X. et al., 2014. Geopolymer prepared with high-magnesium nickel slag:
642 Characterization of properties and microstructure. *Constr. Build. Mater.* 59, 188-194.
- 643 [19] Zhang, Z., Zhu, Y. et al., 2017. Conversion of local industrial wastes into greener cement
644 through geopolymer technology: A case study of high-magnesium nickel slag. *Constr. Build.*
645 *Mater.* 141, 463-471.
- 646 [20] Maragos, I., Giannopoulou, I.P. et al., 2009. Synthesis of ferronickel slag-based
647 geopolymers. *Minerals Engineering*. 22, 196-203.
- 648 [21] Komnitas, K., Zaharaki, D. et al., 2009. Effect of synthesis parameters on the compressive
649 strength of low-calcium ferronickel slag inorganic polymers. *Journal of Hazardous Materials*.
650 161, 760–768.
- 651 [22] Choi, Y.C., Choi, S. 2015. Alkali–silica reactivity of cementitious materials using ferro-
652 nickel slag fine aggregates produced in different cooling conditions. *Constr. Build. Mater.* 99,
653 279-287.
- 654 [23] Dourdounis, E., Stivanakis, V. et al., 2004. High-alumina cement production from FeNi-ERF
655 slag, limestone and diasporic bauxite. *Cement and Concrete Research*. 34, 941–947.
- 656 [24] ASTM C204-11, 2013. Standard test methods for fineness of hydraulic cement by air-
657 permeability apparatus. ASTM International.
- 658 [25] Lamond, J. F., and Pielert, J. H., 2006. Expansive mechanism of magnesia as an additive of
659 cement and concrete-making materials. ASTM International, 169(4).
- 660 [26] ASTM C311, 2013. Standard test methods for sampling and testing fly ash or natural
661 pozzolans for use in Portland-cement concrete. ASTM International.

- 662 [27] AS3582.2, 2016. Supplementary cementitious materials Part 2: Slag-Ground granulated blast-
663 furnace . Australian Standard.
- 664 [28] AS3582.2., 2001. Supplementary cementitious materials for use with portland and blended
665 cement - Slag - Ground granulated iron blast-furnace. Australian Standard.
- 666 [29] Mo, L., Deng, M. et al., 2010. Potential approach to evaluating soundness of concrete
667 containing MgO-based expansive agent. *ACI Materials Journal*. 197(2), 99-105.
- 668 [30] Zheng, L., Xuehua, C. et al., 1991. MgO-type delayed expansive cement, *Cement and*
669 *Concrete Research*, 21, 1049-1057.
- 670 [31] AS2350.5., 2006. Methods of testing portland, blended and masonry cements - Determination
671 of soundness . Australian Standard.
- 672 [32] AS3583.4., 1991. Methods of test for supplementary cementitious materials for use with
673 portland cement - Determination of autoclave expansion. Australian Standard.
- 674 [33] ASTM C109, 2013. Standard test method for compressive strength of hydraulic cement
675 mortars (Using 2-in. or [50-mm] cube specimens). ASTM International.
- 676 [34] ASTM C150, 2012. Standard specification for Portland cement. ASTM International.
- 677 [35] J.J. Brooks, M. Megat, A. Johari, M. Mazloom, 2000. Effect of admixtures on the setting times
678 of high-strength concrete. *Cem. Concr. Compos.* 22 (4), 293–301.
- 679 [36] Erdogan O., Mustafa E. et al., 2016. Utilization and efficiency of ground granulated blast
680 furnace slag on concrete properties – A review. *Constr. Build. Mater.* 105, 423-434.
- 681 [37] Snelson, D., Wild, S. et al., 2011. Setting times of Portland cement–metakaolin–fly ash blends.
682 *Journal of Civil Engineering and Management*. 17(1), 55-62.

- 683 [38] ASTM C618-08a, 2006. Standard specification for coal fly ash and raw or calcined natural
684 pozzolan for use in concrete. ASTM International.
- 685 [39] AS 3972, 2010. General purpose and blended cements. SAI Global Limited.
- 686 [40] ASTM C150-97a, 1998. ASTM specification for Portland cement. ASTM International, 100
687 Barr Harbor Drive, West Conshohochen.
- 688 [41] ASTM C618-98, 1999. ASTM specification for coal fly ash and raw or calcined natural
689 pozzolan for use as a mineral admixture in concrete. ASTM International, 100 Barr Harbor Drive,
690 West Conshohochen, PA.
- 691 [42] Kumar, L., Li, W.Z. et al., 2009. Synthesis, characterization and optical properties of $Mg(OH)_2$
692 micro-/nanostructure and its conversion to MgO. *Ceramics International*. 35, 3355–3364.
- 693 [43] Yu, J.C., Xu, A. et al., 2004. Synthesis and Characterization of Porous Magnesium Hydroxide
694 and Oxide Nanoplates. *J. Phys. Chem.* 108, 64-70.
- 695 [44] Henrist, C., Mathieu, J.P. et al. 2003. Morphological study of magnesium hydroxide
696 nanoparticles precipitated in dilute aqueous solution. *Journal of Crystal Growth*. 249, 321–330.
- 697 [45] Wu, X.F., Hu, G.S. et al. 2008. Synthesis and characterization of superfine magnesium
698 hydroxide with monodispersity. *Journal of Crystal Growth*. 310, 457–461.

699